1968
8-21-75

D2-1558

UCRL-51749

STUDIES OF RADIATION BLISTERING EFFECTS ON VOLTAGE HOLDING

George H. Miley

March 31, 1975

Prepared for U.S. Energy Research & Development Administration under contract No. W-7405-Eng-48

LAWRENCE LIVERMORE LABORATORY
University of California/Livermore

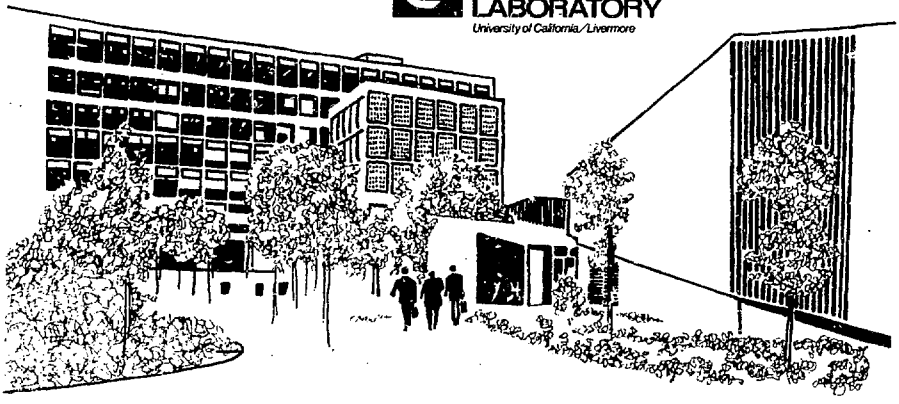

Printed in the United States of America
Available from
National Technical Information Service
U. S. Department of Commerce
5285 Port Royal Road
Springfield, Virginia 22151
Price: Printed Copy $___*; Microfiche $2.25

*Pages	NTIS Selling Price
1-50	$4.00
51-150	$5.45
151-325	$7.60
326-500	$10.60
501-1000	$13.60

Distribution Category
UC-20

LAWRENCE LIVERMORE LABORATORY
University of California/Livermore, California/94550

UCRL-51749

STUDIES OF RADIATION BLISTERING EFFECTS ON VOLTAGE HOLDING

George H. Miley

MS. date: March 31, 1975

Contents

Abstract

The surfaces of niobium and tungsten wires were blistered by 300-keV helium-ion irradiation and then tested for voltage holding. A cylindrical projection-tube technique was employed so that regions of strong electron emission could be observed and later examined with a scanning electron microscope (SEM). Blistering was found to cause significant increases in pre-breakdown currents. However, these currents tend to saturate over a region corresponding to around 200-400 kV/cm surface field such that the ultimate voltage breakdown limit is not seriously reduced. Emission image observations and SEM photographs suggest that, in many cases, parts of the blistered surface are gradually erected by the strong surface fields, but this may not occur until after several arc breakdowns. SEM photographs also indicate that vapor from the anode may play an important part in the breakdown mechanism. Implications of these results to the design of devices important to fusion development, such as direct collectors and ion sources, are briefly discussed. The importance of future *in situ* irradiation-voltage experiments is also stressed.

Introduction

Maintaining high voltages on grid and electrode surfaces is essential for successful operation of both direct-collection units and neutral beam sources in mirror fusion systems. An earlier report[1] describes coaxial grid-cylinder experiments designed to develop voltage breakdown criteria for the design of direct-collectors.* There it was suggested that the criteria be divided into three separate regimes: the *initial* regime, which applies to unconditioned surfaces; the *field-emission* regime, which occurs when "whiskers" are present on partially conditioned surfaces; and the *ultimate* regime, which applies to well-conditioned wires where no evidence of whiskers or field emission occur before the actual breakdown. Conditioning was achieved in these studies by holding the tungsten wires at $\sim$ 1000°C in vacuum for $\sim$ 24 h.

If direct collection and ion sources are to be scaled up to the size and voltage ultimately necessary for fusion reactor operation, then grid surfaces must be conditioned to the extent that voltage holding is better than that exhibited in the initial regime. One possible obstacle to this is that the surfaces in both devices undergo ion bombardment, particularly critical in a direct collector where helium ions (fusion products from burning D-T) can quickly cause blistering of the surfaces. Earlier reports[1-3] postulated that ruptured blisters might cause enhanced field emission via formation of whisker-like projections, as well as initiate arcs through flaking. The present experiments were designed to look into such effects and also to develop some techniques necessary for future studies. Ultimately, it is essential to run *in situ* blistering-voltage tests, but for expediency, the grid wires here were *first* blistered and *then* tested for breakdown. These preliminary observations, in addition to the normal voltage-current measurements, appear essential to understanding breakdown mechanisms.

A projection-tube technique was developed to record emission current patterns associated with blister sites. The tube essentially consists of a glass anode with a fluorescent coating that allowed visual observation of electron currents originating at the wire (cathode) under test. Based on the present experience, it should be possible to design a projection-tube that can be placed in the accelerator beam-line for *in situ* tests. In addition to tracing actual current patterns, the projection-tube greatly simplifies the problem of locating the surface projections or irregularities that cause emission.

*Comments about the application of these criteria to the design of extractor electrodes for ion sources are included in Appendix A. Some preliminary studies of pre-breakdown emission currents from a molybdenum grid used in a LBL MATTS-type source are given in Appendix B.

The Apparatus and Projection Tube

Breakdown tests were performed with the grid wires under test biased at a high negative potential relative to the cylindrical anode (see Fig. 1). This arrangement is essentially the same as that employed in the earlier studies, and it and the voltage-current measurement techniques are discussed in detail in Ref. 1. A new power supply was used in the present arrangement so that higher voltages and currents could be achieved. Also, the vacuum chamber and holder were modified to allow larger anode cylinders and to make it easier to insert new wires and anodes (e.g., compare Fig. 1 here to Fig. 3 of Ref. 1). Also the ballast resistor and adjustable parallel capacitor were mounted such that they could be changed to vary the circuit parameters. Finally, due to x-ray production at the high voltages used here, it was necessary to enclose the entire bell jar in a lead shield provided with a lead glass window for viewing.

This coaxial arrangement has three major advantages. First, very high electrical fields can be obtained at the surface of the grid wires with a modest power supply. Second, this represents a "natural" configuration for collector and ion-source studies, since grid wires are involved in both. Third, the use of a wire-type cathode makes it straightforward to condition the wire surfaces with a heat treatment via resistive heating with a dc current. Mounting wires for ion bombardment and subsequent electron microscope studies posed some mechanical problems, but this was a minor annoyance.

The projection tube represented the most important new part of the apparatus. This tube consisted of a glass cylinder internally coated with an aluminized cathode-luminescent phosphor. Patterns created by electron currents from the grid under test could be observed as bright glowing spots on the phosphor. The projection tube was designed to replace the stainless steel anodes used previously (see Fig. 2). Two sizes of tubes were built having i.d.'s of 2 in. and 4 in. respectively, both having a length of 8 in. They were constructed using special coating processes developed for the purpose by R.M. Kinkaid of EG&G Co. under

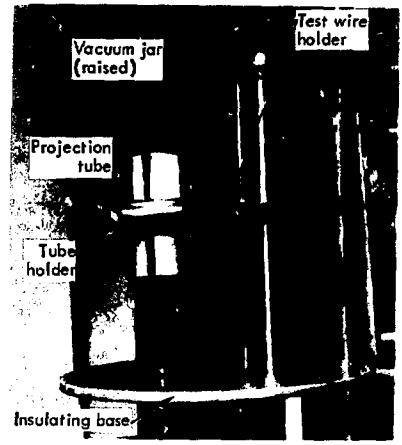

Fig. 1(a). Photograph of the voltage test apparatus with vacuum bell jar raised.

contract with Lawrence Livermore Laboratory.[4] About 1 to 2 mg/cm^2 of P-11 type phosphor, coated with 1 to 2000 Å of aluminum, was employed. Electrons of order of 1 keV energy had sufficient energy to penetrate the aluminum and create a visible spot on the phosphor. The decay time for light from the phosphor was of order of 0.1 msec. The conducting aluminum surface acted as the anode and was electrically connected to the external circuit through electrodag bands painted on the outer glass surface such that contact with the anode holder was established (see Figs. 1(b) and 2).

The projection tube technique is not new. It was originally employed in the late 1930's for studying thermionic emission, but it was not until 1964 when Brodie and Weissman[5] adopted the technique that it was used for breakdown studies. More recently, Maley[6] demonstrated the usefulness of the technique when he studied various conditioning techniques.

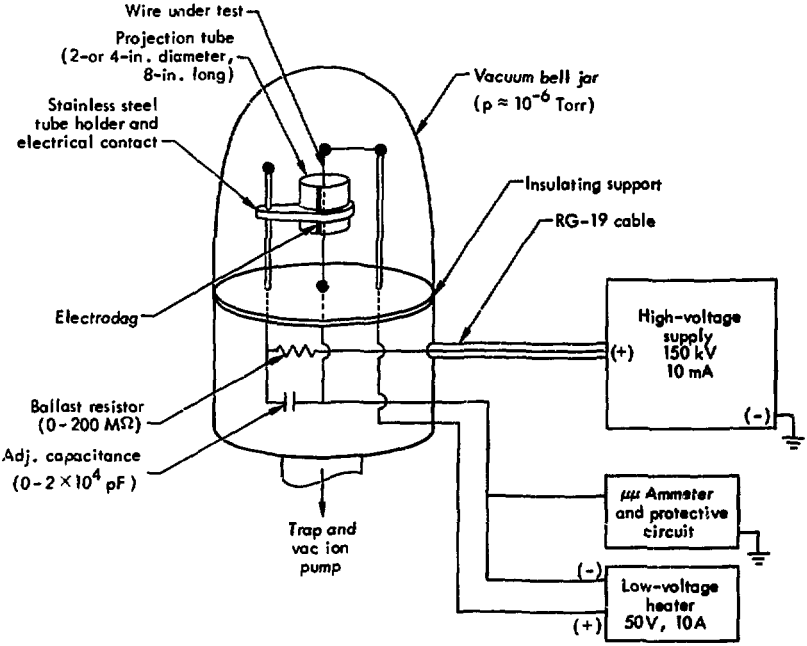

Fig. 1(b). Schematic illustration of the apparatus.

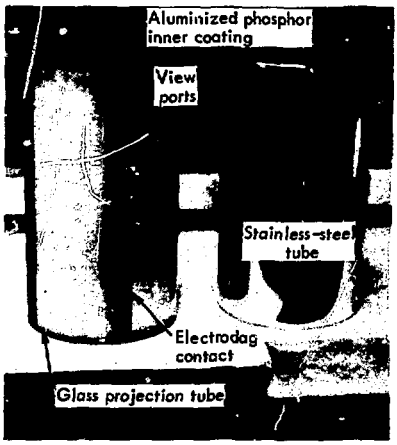

While the construction of the present tubes appears to be quite similar to those in these earlier references, considerable care was taken to insure good bonding of the coatings. This made it possible to extend present studies to the point where repeated breakdown occurred. (Previous studies were limited to pre-breakdown current observation, apparently for fear of damaging the tube.) Some damage occurred as the experiments progressed, including cracking of the glass, but many breakdowns were observed without completely destroying a tube.

Fig. 2. Photograph of the 4-in. diameter projection tubes and a corresponding stainless-steel anode. The smaller 2-in. diameter projection tube (not shown) used in some experiments was similar in construction.

Calibration Studies

The present studies introduce several fundamental questions: Does breakdown with the projection tube differ significantly from the previous studies of Ref. 1 that used the stainless-steel anode? How does breakdown with an electropolished (or chemical polished) grid wire differ from that with the untreated (commercial) wire used previously in Ref. 1? How does breakdown with niobium wires compare with tungsten? (Most experience with blistering involves niobium, since it is a prime prospect for fusion reactor first walls. Thus it was used for most of the present studies although tungsten is generally envisioned for grid-wire construction.)

We obtained approximate answers to these questions, adequate for the present. If such experiments are continued, however, more precise studies must be done. We will briefly consider each question in turn.

PROJECTION TUBE EFFECT ON BREAKDOWN

Breakdown strengths reported in following sections for normal (unblistered) wires and projection tubes generally agree with earlier results for stainless-steel anodes.* This is not surprising since the material used for the anode is not thought to play a strong role in breakdown.[1] Some small differences may exist, but precision comparisons were not considered necessary for present purposes.

*A most noticeable effect was the formation of a stable low-voltage discharge following initial arc breakdown. In this mode, most of the voltage drop occurred across the ballast resistor rather than the vacuum gap. As discussed later, the discharge is thought to be maintained by evaporization of aluminum from the projection tube coating, resulting in a low-density plasma. It should be stressed, however, that the discharge did not occur until *after* breakdown, hence the pre-breakdown currents and breakdown limit were not affected.

EFFECT OF POLISHING WIRE SURFACES

Earlier studies[1] with tungsten wire used commercial stock* without special surface treatment such as electropolishing. This was done since commercial wires are anticipated for use in actual devices such as direct collectors. However, Scanning Electron Microscope (SEM) photographs showed that the surfaces of such wires are generally too rough to permit systematic blister studies. Typical niobium wire surfaces have a particularly coarse structure, as shown in Fig. 3. Tungsten wire, shown in Fig. 4, has distinct grooves, but is more regular than niobium.

Tungsten can easily be electropolished using standard techniques. Less information is available on niobium treatment, so two techniques were used: electropolishing and chemical polishing.

Polishing turned out to be rather tedious, largely due to the necessity of maintaining very uniform dimensions over the diameter and length of the wire. This was particularly difficult because it was found necessary to remove considerable thicknesses of the material before the die grooves were smoothed. For example, it was necessary to polish a 10-mil wire to less than 5-mil diameter to obtain a satisfactory surface. To do this, a special rig was built so that the wires could be continuously rotated in the polishing solution. This usually maintained the diameter over the test length (about 6 in.) within ± 0.1 mil.

A 3-mil diameter tungsten wire formed by electropolishing from 10-mil stock is shown in Fig. 4. Comparable niobium wires employing chemical and electropolishing are shown in Fig. 5. While the surfaces are far from perfect (also note the enlarged niobium scans in Fig. 6), they were thought to be satisfactory for the present blistering experiments.

*All tungsten and niobium wire used in the present as well as earlier experiments were high-purity (> 99.98%) stock.

Fig. 3. Standard niobium wire is characterized by a particularly rough surface. A distinct structure is superimposed on the characteristic die grooves.

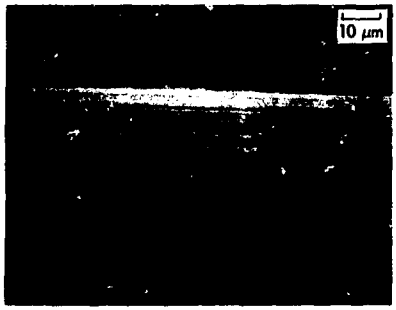

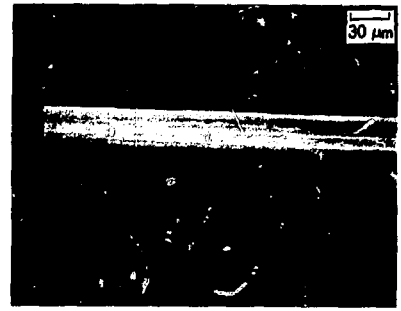

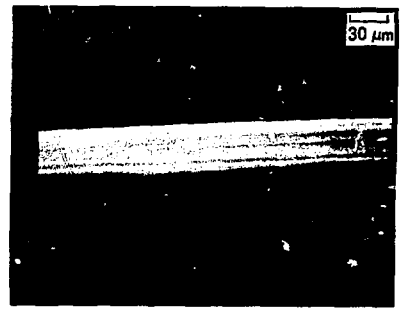

Fig. 4. Die grooves are clearly visible in the upper photo of standard tungsten wire. After electropolishing the grooving is smoothed (lower photo).

Fig. 5. Niobium wire after polishing (electropolishing, upper photo; chemical polishing, lower photo). While some gross die structure remains, the fine structure is removed.

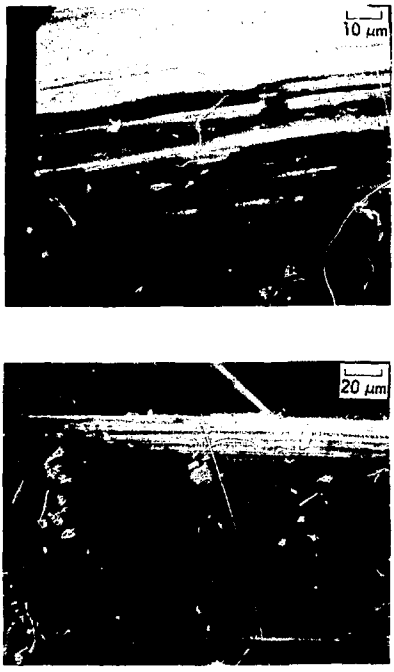

Fig. 6. Enlarged SEM photos of polished niobium wire (electropolish, upper photo; chem-polish, lower photo).

As discussed later, even the die grooves on commercial wire generally represent "rounded" protrusions and, as such are not an important factor in voltage breakdown. (Sharp projections on the surface, having length-to-diameter ratios of 10 or greater[1] are necessary to obtain enhanced field emission which appears to play a key role in breakdown from tungsten and niobium wires.) Thus the main consideration was to obtain sufficient smoothing to permit a "normal" blister pattern.

Two additional observations are pertinent. Scans of the polished surfaces indicated an occasional protrusion of the type shown in Fig. 7. Since microprobe analysis indicated the presence of a calcium-silicate, it was concluded that this was some debris remaining after the polishing procedure. Such protrusions could play an important role in breakdown, so subsequent wires were given even more extensive washing in CCl_4 and distilled water after polishing. A second point that deserves continued study is heat treatment, used successfully in both the earlier and present studies to condition surfaces. Figure 8 clearly shows a smoothing of the tungsten grooves plus the formation of a

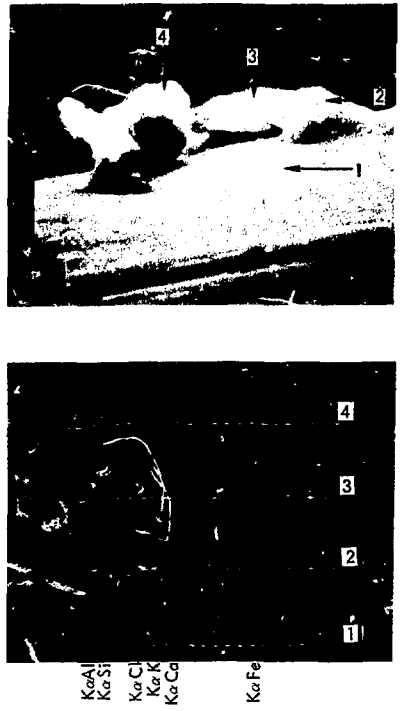

Fig. 7. Some foreign matter remaining after polishing. As seen from the microprobe traces, the protrusions contain a calcium silicate along with phosphates. (KαAl indicates the location of Kα emission from Al, and so on.

Fig. 8. Optical microscope view of tungsten wire after heat treatment for 2 hours at 1125°C. Smoothing of the groove structure plus grain formation is observed.

visible grain structure. This is not well understood, since the temperatures involved (1125°C for 2 h) would seem to be too low to have such a pronounced effect.* Still, a marked improvement in voltage holding is obtained by such treatment.

The effects of various surfaces are compared in the current-voltage plots of Fig. 9. The pre-breakdown current before heat conditioning was large for the untreated and electropolished tungsten. While the current from the electropolished wire was somewhat lower, its breakdown voltage was virtually identical to that for the unpolished wire. After heat conditioning, both wires exhibited lower currents, but with an exponential increase characteristic of field emission. While the currents at breakdown varied somewhat, the breakdown voltage again remained comparable for the two wires.

These results indicate that smoothing the surface by polishing can reduce the initial emission currents. However, since the breakdown voltage is not noticeably changed, the surface structures causing ultimate breakdown apparently are not removed. These structures (or possibly clumps) may be drawn from the surface by electric field forces and hence be independent of the initial roughness. Heat conditioning is shown to be much more effective in reducing currents and raising breakdown voltages than polishing. Consequently, prior history (i.e., polishing, etc.) is essentially eliminated as a variable after thorough heat conditioning.

BREAKDOWN WITH NORMAL NIOBIUM WIRES

Since previous studies[1] used tungsten wires exclusively, runs with both a standard and a chemical-polished 5-mil niobium wire were performed. As with the wires in Fig. 9, some variations were noted before heat conditioning, but after that stage, the V-I curves and breakdown voltages were comparable with tungsten. (Field emission patterns observed on the projection tube were also comparable, suggesting similar breakdown mechanisms.) Some minor differences in behavior may exist, but for subsequent studies of blistering, this rough comparison was considered adequate and further tests were not attempted.

*Very-high-temperature ($\gtrsim 2000$°C) annealing has been reported as a good way to smooth tungsten surfaces and remove die marks; however, the wire becomes quite brittle. This would not be satisfactory for grid operation due to the electric field forces involved, hence only low-temperature conditioning has been considered.

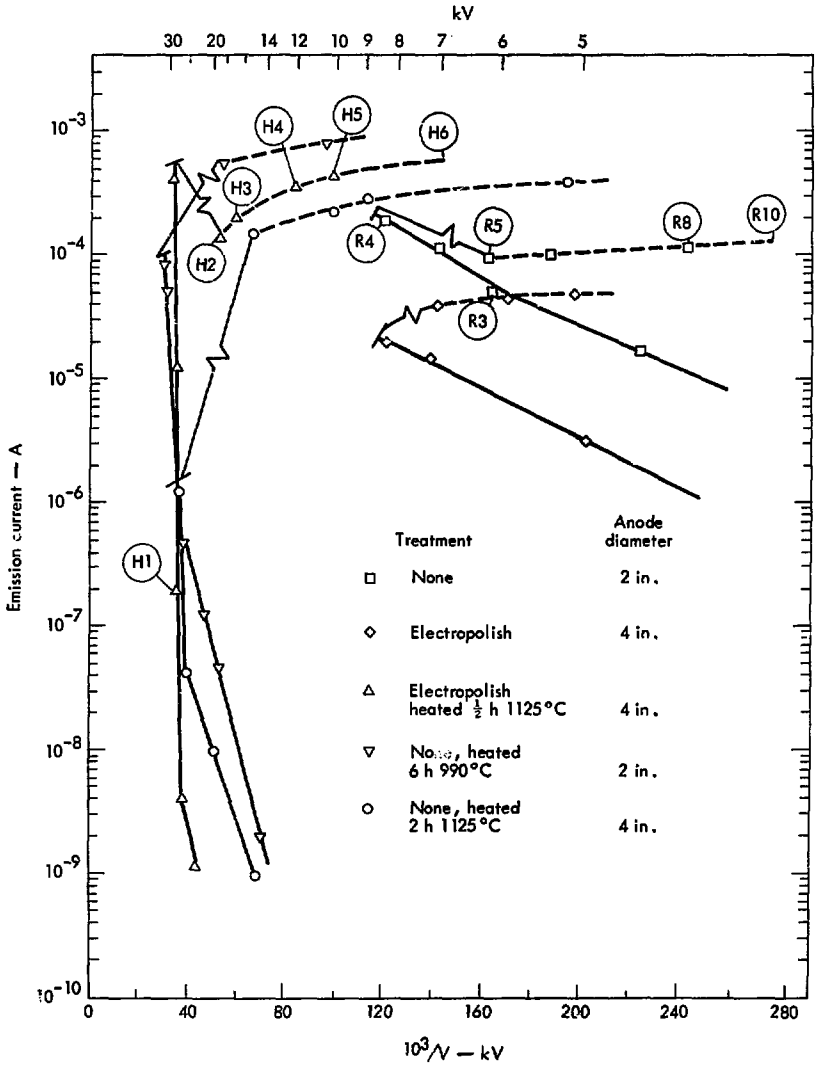

Fig. 9. V-I curves for polished and unpolished tungsten wire. (Slash = arc breakdown point.) Projection tubes with two different diameters were employed, but theory[1] indicates that the current and breakdown should not depend strongly on tube diameter. Due to the ballast resistor employed, a stable low-voltage discharge could be maintained after the actual breakdown (indicated by dashed lines). Circled symbols show points where projection tube photographs (Fig. 10) were taken.

PROJECTION-TUBE OBSERVATIONS WITH NORMAL WIRES

A typical sequence of emission images observed with the projection tube during tests of the normal (unblistered) wires is shown in Fig. 10.

The upper series of photographs involved an unconditioned but polished tungsten wire. Several bright emission spots, partly obscured by the tube holder at the center of the tube, are observed in photo R4 just prior to arc breakdown (refer to Fig. 9). These emission sites appear to have been destroyed by the breakdown since that area of the tube is dark in photo R5. By this point, and in subsequent photos, the device has entered a stable low-voltage discharge mode where the main voltage drop occurs over the 200-MΩ ballast resistor (see Fig. 1 (b)) rather than across the gap itself.* In this regime, as the power supply voltage is increased, the discharge current increases, causing a larger voltage drop across the ballast resistor. This in turn reduces the actual voltage across the inter-electrode gap, leading to the characteristic "negative" resistance portion of the curves shown by dashed lines in Fig. 9.† During this phase, as seen from photos R5 to R10, the number of emission sites increases rapidly with increasing current.

The second series of photographs in Fig. 10 (series b) illustrates the behavior of a heat-conditioned 2-mil tungsten wire. As seen by again referring back to Fig. 9, this wire achieved a much higher voltage before breakdown. In this case, only one spot (photo H1) was observed before breakdown, and the associated surface projection was apparently destroyed upon arcing, since the spot disappears in photo H2. Again a rapid increase in the spot density is observed in the low-voltage discharge mode. In this case, a smaller ballast resistor (10 MΩ) was employed, so the discharge currents were roughly an order of magnitude larger than with the electropolished wire. As the currents approached a milliampere, microdischarges tended to occur, causing the spot pattern to break into a fine structure plus soft glow as seen in photo H6.

Post-breakdown behavior, represented by the low-voltage discharge regime, was not of direct interest to the present work, but several comments are in order. While the mechanism involved is not fully understood, it seems reasonable to assume that the discharge is sustained by localized plasma-arcs feeding on vaporized aluminum from the projection tube surface. This could explain the increase in spot density with current despite a lower net field at the wire surface. In the low-voltage mode, sufficient aluminum vapor may exist to allow arcs from whisker sites where the fields are normally too small to cause much emission. As the current increases, and some microdischarging occurs, more aluminum is vaporized, creating yet more emission sites.

Finally, we note that the correlation of spot density with emission current in the low-voltage discharge regime was reasonably consistent, independent of the type of wire involved. This is illustrated in Fig. 11, where the spot density vs current is shown for tungsten, niobium, and molybdenum. The spot density appears to increase somewhat faster than predicted by a linear relation with current. Still, in view of the variations in spot sizes and intensities, the proximity to linear behavior is quite striking.

*Note that had the ballast resistor not been present or a smaller one used, the breakdown arc would have drawn sufficient current to trip the circuit breakers in the power supply and terminate the run. *Voltage breakdown*, then, is defined as the point where arcing results in a switch to a low-voltage arc discharge, independent of whether or not this discharge can be sustained by the power supply. At that point the inter-electrode gap has essentially changed from an insulating to a conducting element in the circuit.

†The voltage of Fig. 9 corresponds to the vacuum gap, and as seen from the figure the current increases although this voltage drops. A similar situation is encountered in glow-discharge plasma tubes where a ballast resistor is employed to stabilize the discharge. There the corresponding region of the V-I curve is described as having a "negative" resistance.

a) Electropolished 2-mil tungsten (no heat conditioning).

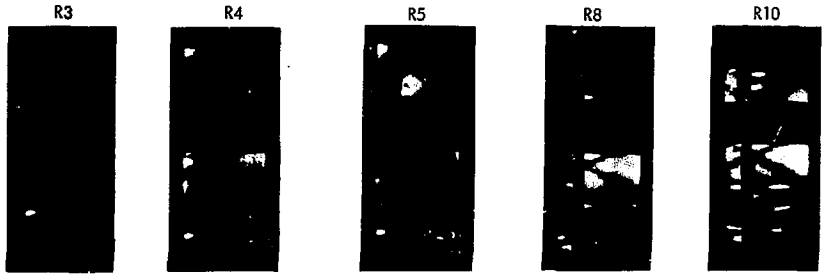

b) 2-mil tungsten after conditioning at ~990°C for 6 hours.

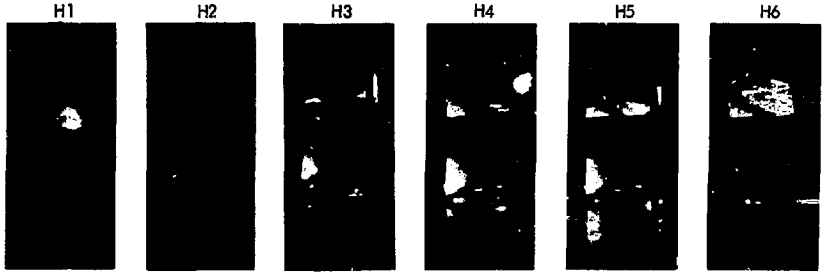

Fig. 10. Sequence of projection-tube patterns observed with normal 2-mil tungsten wire. Numbers by each photograph refer to points on the current-voltage curves in Fig. 9.

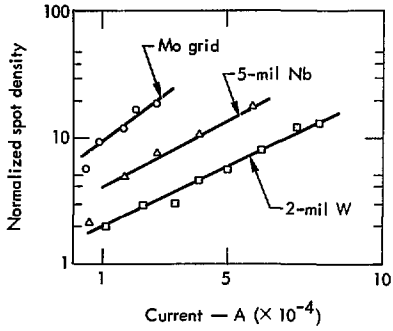

Fig. 11. Variation of emission spot density with current for several wires in the low-voltage discharge regime.

INTERPRETATION OF EMISSION IMAGES

The emission spots observed throughout these studies were inevitably elliptical.* This is consistent with projection-tube observations by others, and Brodie[7] explains this in terms of electron trajectories in the cylindrical-field configuration. He finds that the length of the minor axis of the spot is a measure of the height of the whisker where the field emission

*On several occasions, long, thin (approximately vertical) streaks were also observed, e.g. see photo W17 included later in Fig. 14. Streaks typically shifted with changes in voltage (or with time at a fixed voltage), suggesting movement of projections on the wire surface.

originates. To a good approximation, the whisker height h is

$$h \approx R_1 \left\{ \exp[(r_o^2/R_2^2) \cdot \ln (R_2/R_1)] - 1 \right\} \qquad (1)$$

where R_1 is the radius of the wire, R_2 is the inner radius of the projection tube, and r_o is the half length of the minor axis of the elliptical image. For example, $r_o \approx 0.25$ cm for the larger of the two overlapping images* in photo H1 of Fig. 10. (This spot is selected since, as noted earlier, it was associated with an arc breakdown.) Then, from Eq. (1), the whisker height is about 0.5 μm or 5000 Å. Assuming that, as found earlier,[1] the electric field enhancement involved is of the order of 100, a height-to-diameter ratio of around 10 is required,[7] indicating a whisker diameter of the order of 500 Å.

This example is reasonably typical of the present observations. Spot sizes varied from case to case, however, and it is estimated that whisker heights generally ranged from 100 to 50,000 Å. For comparison, Brodie[7] reports whiskers on nickel wires ranging from 700 to 100,000 Å in height.

This illustrates the importance of using a projection tube to locate emission sites prior to scanning with the SEM. The debris shown earlier in Fig. 7 is about 10 times the height of the largest whisker indicated above. If the surface is scanned at low magnification (< 1000) the smaller whiskers would be difficult to see. Scanning at high magnification is difficult and time-consuming. Further, as seen from Fig. 9, there may be only one or two critical whiskers on the entire length of wire that lead to breakdown, and these can easily be overlooked in a general scan. These comments raise doubt for the argument that, since whisker structures have not been observed on wires before testing, they must be pulled up by the field itself. Still, the sudden appearance of spots at voltages above the 1-2 kV required to form a visible image on the projection tube supports the field argument.

*The shape of these spots was quite clearly visible in the original color photographs. Unfortunately much of the contrast was lost in the black and white reproductions necessary for the present report.

REFERENCE WHISKER EXPERIMENT

To obtain further information about the operation of the projection tube, an attempt was made to form a "reference" whisker of known dimensions on the wire surface. While quantitative results were not obtained, some of the observations are of interest in the interpretation of the later blister experiments.

With the time and facilities available, it was not possible to grow a realistic whisker. (Techniques are available to do this, and it would appear worthwhile to repeat the experiment with "better" whiskers in the future.) A 1/2-mil stainless steel filament was welded onto a 5-mil tungsten wire, as shown in Fig. 12. (Attempts failed to weld niobium or tungsten filaments.) With a height-to-diameter ratio of about 20, the filament was thought to offer strong field enhancement.

Voltage-current measurements and projection tube photos for the wire experiment are shown in Figs. 13 and 14, respectively. Run 1 was terminated prior to breakdown since relatively large currents were obtained without an image on the projection tube at the reference whisker height. Thus a mild surface conditioning was thought to be advisable and the wire

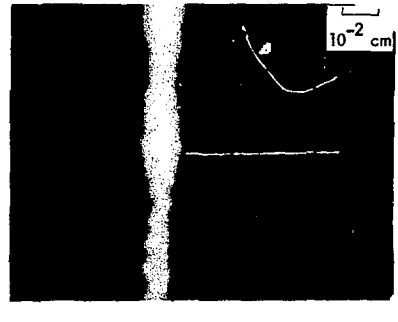

Fig. 12. The "reference" whisker formed by welding a 0.5-mil stainless steel filament to a 5-mil tungsten wire. The filament extended out from the wire in two directions (forming approximately a 135° angle between prongs) as is barely visible from the dark shadow on the left.

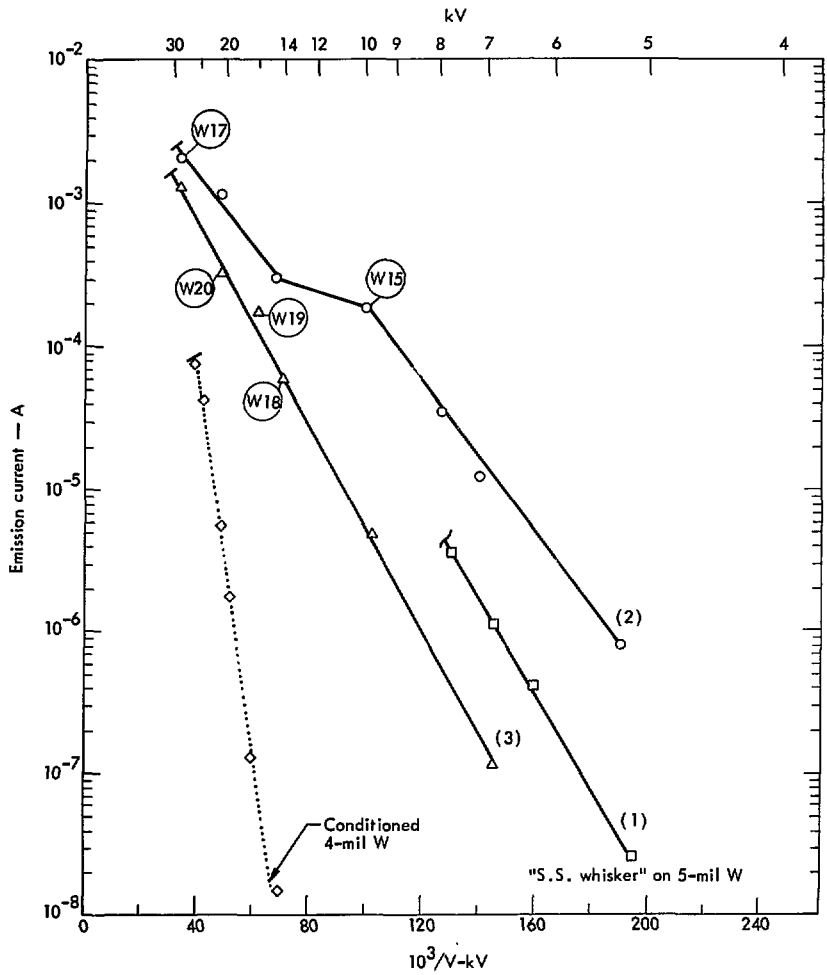

Fig. 13. Current-voltage curves for runs 1, 2 and 3 (parenthesis) with the "reference" whisker. For comparison, the typical 4-mil tungsten curve is again shown. The bars indicate arc breakdown while wavy cross line indicates shutdown prior to arcing.

a) Reference whisker run 2 (following partial run without arc and mild heat conditioning).

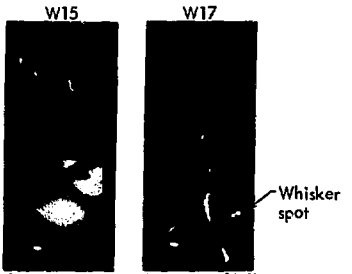

b) Reference whisker run 3 (following termination of run 2 via arc).

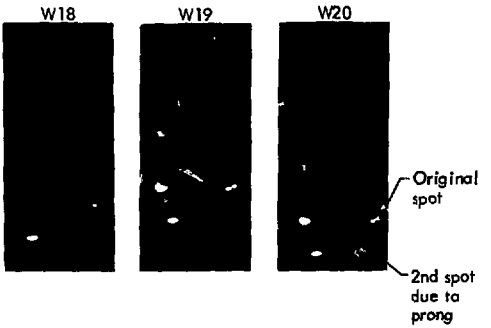

Fig. 14. Projection-tube images from reference whisker runs. Photo numbers refer to Fig. 13.

was held at a low temperature ($\lesssim 700°C$) for one hour. This temperature was thought to be too low to damage the whisker. Still, in run 2, as seen from photo W15, a dull glow developed in the tube and the initial emission spot was not at the whisker height. However, a spot did develop at the correct location just prior to arcing (photo W17). In the third run, the same spot pattern appeared again at low voltage, and then a new spot was added at the whisker location (photos W19 and W20). [This spot was in the correct position to represent the second prong of the reference whisker (recall Fig. 13)]. After this run (terminated by an arc), distinct spots associated with the reference whisker were no longer visible. Consequently, the wire was removed for examination, but the whisker was no longer clearly visible under a low-power optical microscope. Indeed, a SEM photo of the weld area, shown in Fig. 15, indicated that the whisker filament had broken or melted off and the remaining portion was bent over near the surface. The small (*about 4-μm diameter*) balls visible on the whisker stub were identified by microprobe analysis as aluminum, indicating transport of considerable quantities of vapor from the projection-tube surfaces. (Telltale aluminum balls were observed many times in subsequent work, as discussed later.)

Several points stand out in this study. First, despite the presence of an exceptionally large reference whisker, some field emission occurred at other points along the wire. The whisker itself did not cause a premature breakdown as might have been anticipated (note runs 2 and 3 in Fig. 13). Concurrently, the whisker spots did not appear as soon as expected nor are the sizes consistent with Eq. (1).

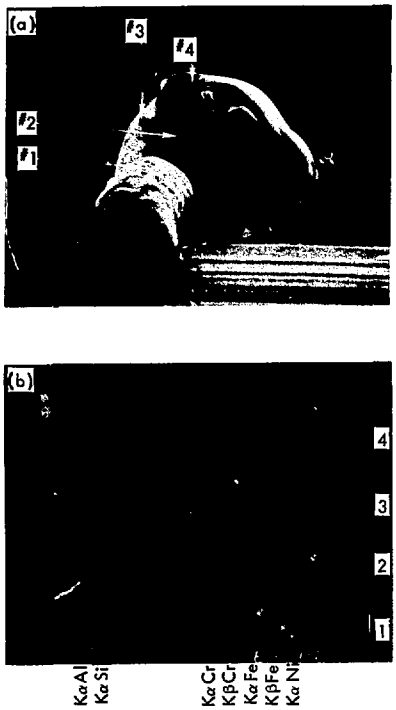

Fig. 15. Reference whisker after voltage breakdown. Microprobe analysis at bottom indicates a significant percentage of aluminum in ball at location 3.

The whisker may have been damaged early in the experiment so that that data recorded only applies to the stub shown in Fig. 15. (This proposition would be consistent with the large amounts of aluminum transferred to the stub, indicating considerable arcing must have occurred there.) Clearly, further experiments of this type are needed to unravel the mechanisms involved.

An intriguing, perhaps coincidental, aspect of these observations is that spots associated with blistered wires (discussed later) often did not appear at low voltages either. Also, as happened with the reference whisker, it appears that pre-breakdown currents and microdischarges easily destroyed emission sites caused by blistering.

SEM PHOTOS OF EMISSION SITES AND ARC CRATERS ON NORMAL WIRES

Following the runs shown earlier in Fig. 9, a 2-inch length was cut out of the normal (unblistered) 2-mil tungsten wire where several large emission sites appeared on the projection tube. Typical photographs from SEM observations of this section are shown in Figs. 16 through 20.

In general, two types of arc craters were observed:

- Massive craters (diameter of order of 30 μm – Fig. 16)
- Small "drill-hole" craters (diameter of order of 0.5 to 2 μm) – Figs. 19 and 20).

The massive craters are similar to those reported by Brodie (see Fig. 39 of Ref. 7) during his nickel-wire studies. He attributed these to arcs initiated by whisker blowup. There do not appear to be any previous observations of the small drill-type craters, however.

A possible explanation for the existence of two markedly different types of craters is that the larger ones are associated with whisker-initiated breakdown while the drill-hole type originate from small clumps on the surface shown in the top photo in Fig. 19. The origin of these clumps is not known. They were not observed on wires prior to voltage tests; thus, they may be debris from other arcs (note the small clumps around the arc of Fig. 20) or material transported to the wire from the anode.

Several other interesting features are visible in these photographs. In Figs. 16 and 17, a distinctive structure occurs around the edge of the large crater. In Fig. 17, a bent whisker-like formation with a ball on its end is clearly visible. The microprobe analysis of the ball confirms the presence of aluminum, indicating that this structure played a part in prebreakdown emission and/or the arc. (No aluminum was found on the wires before voltage tests. Thus, as noted earlier, any aluminum must have been transported from the projection-tube liner.) The exact size of the bent structure is hard to determine due to the angle of the photograph. Its diameter appears to be about 8000 Å and the height could easily be 5 to 10 times this. This falls close to the upper limit of whisker sizes estimated earlier.

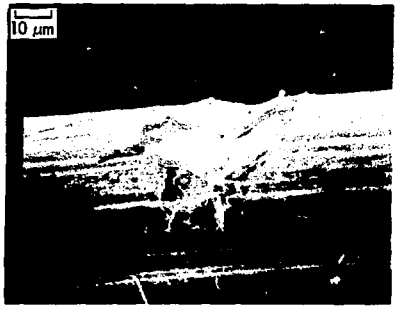

Fig. 16. Massive crater due to breakdown to 2-mil tungsten wire. Lower photo is an enlargement of the projection on right edge of crater.

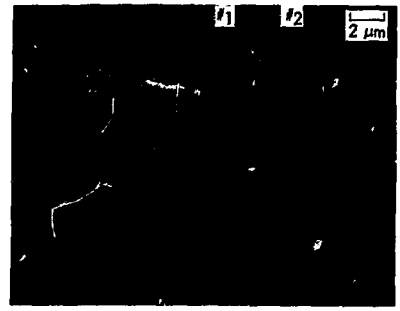

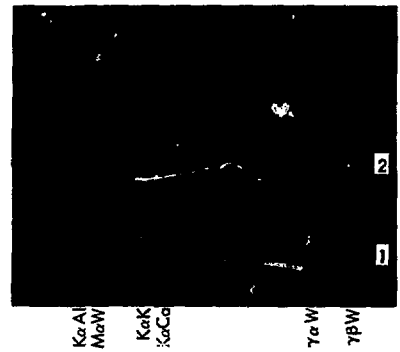

Fig. 17. Bent whisker-ball formation on the edge of the massive crater of Fig. 16. Microprobe analysis of formation (lower trace) indicates presence of aluminum and potassium-calcium (vs. standard substrate of upper trace). Another bent whisker-ball structure on the edge of a crater on niobium wire is shown later in Fig. 25.

Fig. 18. Bump-like structure on 2-mil tungsten after breakdown, thought to be base of evaporated whisker.

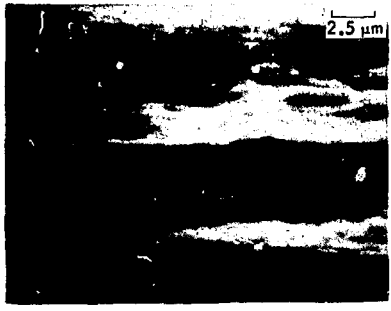

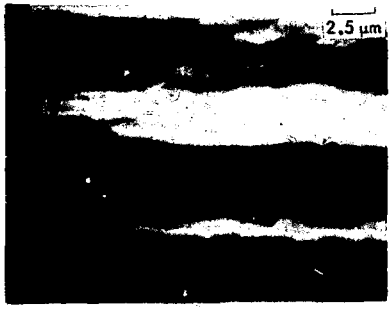

Fig. 19. The small holes "drilled" by arcs on 2-mil tungsten (lower photo) may originate with loose surface material shown in top photo.

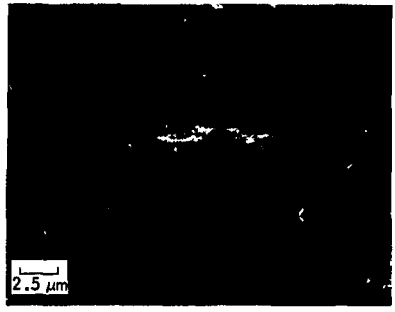

Fig. 20. Another small arc crater on 2-mil tungsten.

This whisker could have been present before the arc, or it may have formed as a result of melting action near the edge of the crater. The latter is a good possibility since projection-tube observations indicate that arcs frequently create new emission sites near the original arc site.

Another structure found near an emission site is shown in Fig. 18. While there is no direct evidence that this bump-like formation was involved in arcing, it could conceivably be the base of a vaporized whisker.

A niobium wire was also sectioned in the region near a particularly bright image spot and examined with the SEM. A large projection with a telltale aluminum ball was located as shown in Fig. 21. The rugged edges, clearly visible on this formation, suggest that it may have been pulled out of the surface, possibly by electric field forces. Its thickness, of order of 10^4 Å, is comparable with the crater-whisker shown earlier in Fig. 17, although the origin of the two seems to be quite different.

COMMENTS ABOUT WHISKER-BALL FORMATIONS

The aluminum balls observed on the cathode projections (or whiskers) in the preceding photographs are attributed to the condensation of aluminum vapor on these points, the vapor originating from the aluminum coating on the projection tube (anode). As stated earlier, this signifies that these particular whiskers were involved in strong emission currents or arc discharges to the anode. The fact that they were located

Fig. 21. Large whisker-ball observed on niobium wire.

by examining regions on the surface identified with strong image spots on the projection tube adds further indirect evidence to this view.

The exact mechanism involved in the aluminum transport and the role that it plays in arc breakdown is not entirely clear, however. The ball in Fig. 21 seems to have been associated with pre-breakdown currents since the projection shows no sign of arc damage. Conversely, the ball in Fig. 17 may be connected with the arc process that created the crater in that photo.

The tip of a whisker would seem to be quite hot (compared to the surrounding surfaces) due to field emission currents, so it is not clear why vapor condensed in this location. The transport of significant amounts of anode material to the cathode is not a new observation, but ball-like structures have not previously been reported. In this respect, the experiments by Davies and Biondi[8,9] are perhaps the most definitive with regards to the present work. Using a resonance-line absorption technique, they have established that for copper electrodes, neutral copper vapor is formed in the interelectrode space *before* the current increases sufficiently to cause breakdown. (Vapor was typically detected a fraction of a microsecond before breakdown.) The mechanism that they postulate to explain this is that material (termed a macroparticle) torn from the anode is subsequently vaporized by electron bombardment as it traverses the interelectrode space. The only electron currents dense enough to do this are associated with field emission from whisker sites. However, the macroparticle is probably aligned with these currents since it is likely to be formed in the first place by local heating of the anode by field emission currents.

Several points are of interest in relation to this theory. Davies and Biondi estimate that an average copper vapor density of about 3×10^{17} atoms/cm^3 would be required to ultimately create a breakdown arc (or discharge). This in turn suggests macroparticles of radii larger than about 8 μm are involved. These values should also provide an order of magnitude estimate for aluminum which is of interest to us.

The aluminum balls in Figs. 17 and 21 have radii of about 1 μm and about 3 μm, respectively. If the atoms represented were distributed in a cylindrical volume of length equal to the interelectrode gap and a cross-sectional area typical of the projection tube spots ($V \approx 0.5$ cm^3), the vapor density would be about $10^{12} - 10^{13}$ atoms/cm^3, well below the critical value indicated earlier. This may be reasonable, since, had the vapor exceeded the critical value, the subsequent arc breakdown would have destroyed the whisker. (It was only possible to photograph survivors!) This suggests that a low-current arc or microdischarge occurred, but the associated vapor-plasma density was too low to sustain an arc current of the magnitude required for complete breakdown. Indeed, microdischarges (short of full discharges) are not uncommon. In fact, such discharges no doubt cause changes in intensity of projection tube spots and the occasional disappearance of some spots prior to final breakdown.

We stress, however, that the microdischarge explanation for ball formation is entirely based on circumstantial evidence. Extensive detailed studies, including line absorption measurements such as used by Davies and Biondi, are necessary to better understand the phenomenon.

Breakdown Experiments with Blistered Wires

As summarized in Table 1, three niobium and two tungsten wires were exposed to an intense helium beam in order to create blistered areas. This was done at the Sandia-Livermore Laboratory accelerator using a current of about 6.3×10^{14} helium ions/cm^2-sec at 300-keV to accumulate a total dose of 4×10^{18} He/cm^2. This accelerator facility is the same one used in the continuing implantation experiments at Sandia (see, for example, Ref. 10).

A 20-inch length of the test wire was coiled and mounted on a special holder* such that a single strand (roughly equal length from either end) was in the helium-ion beam. Thus a region about 1/2 cm long was blistered on one side of the wire. The coiled wire could not be placed in an SEM without damaging it, so the area was viewed under a low-power microscope simply to confirm blistering. The wire was then taken to LLL and mounted in the breakdown apparatus. Care was taken to locate the point on the projection tube next to the blistered area. Information about the blisters was obtained later from SEM photographs of sectioned portions of the wire after arcing. We will briefly describe results from each wire.

*Screw clamps were set about 1/2-inch above and below the implantation area. Unfortunately, the clamps perturbed the wire surfaces slightly, and it is thought that this contributed to some of the emission spots observed outside of the blistered region.

3.2-mil CHEMICALLY POLISHED NIOBIUM

Voltage-current curves, projection tube images, and SEM photos for this wire are shown in Figs. 22, 23, and 24, respectively. From the last figure, it appears that the implantation peeled off regions of order of 10 μm in diameter, leaving only rough edges folded back around the edges of the blistered-flaked area. The depth of the flaking cannot be determined from the photographs, but it is expected to be of the order of the range of the 300 keV He ions (approximately 30 μm). The rough edges appear to project as much as 5 μm. (Note that these dimensions could lead to a large length-to-thickness ratio, hence possible field enhancement.)

As seen from Fig. 22, during the first run the emission current initially exhibited an exponential rise characteristic of field emission. However, a plateau occured at about 10^{-4} A where increases in the voltage from around 8 to 13 kV caused little increase in current. At about 13 kV, the current again increased exponentially until breakdown. Such a plateau region had not been observed earlier[1] with normal wire, but it characteristically appears in all initial runs with blistered wire. Before speculating on its origin, it is instructive to examine the projection tube photographs. The prominent cluster of spots visible in photos L6 through L17 were at the location

Table .. Summary, Irradiated Wires.

Wire	Prior treatment[a]	Diameter (mil)	Type of irradiation damage[b]
Niobium	Chem. polished	3.2 ± .2	Scaly flaking (Fig. 24)
	Electropolished	4.2 ± .2	Complete flaking (Fig. 27)
	Electropolished	6.0 ± .1	Cracked blisters (Fig. 30)
Tungsten	Electropolished	4.9 ± .1	No visible damage
	Electropolished	5.1 ± .1	Porous, melted appearance (Fig. 31)

[a]Starting from 10-mil diameter, high-purity (>99.9%) wire in all cases.

[b]While all wires received similar implantation, differences in blistering occurred due to small variations in location in the ion beam and different temperatures (not controlled).

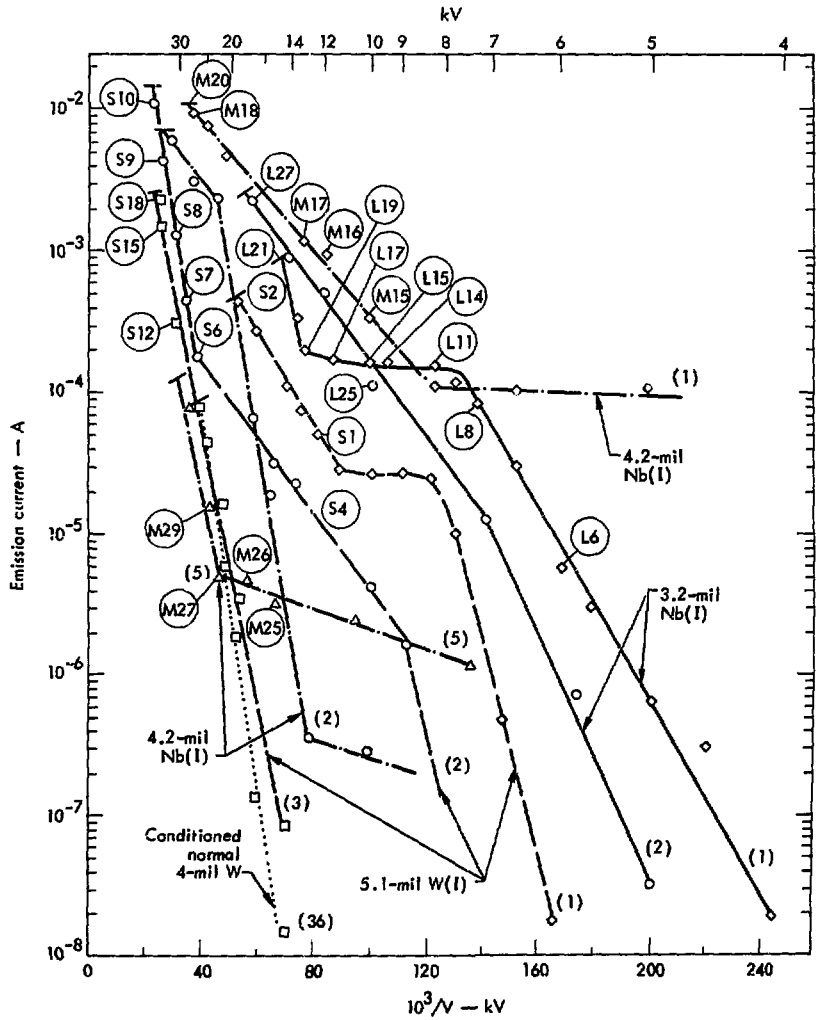

Fig. 22. Current-voltage plots for runs (run nos. in parentheses) of the blistered 3.2-mil niobium wire [Nb(I)], 4.2-mil Nb(I) wire, and 5.1-mil tungsten [W(I)]. For comparison, a typical curve for normal (not blistered, but conditioned by heat treatment) 4-mil tungsten is included. Circled symbols identify time of photos in Figs. 23, 26 and 32. (I) is used to denote irradiated (blistered) wire.

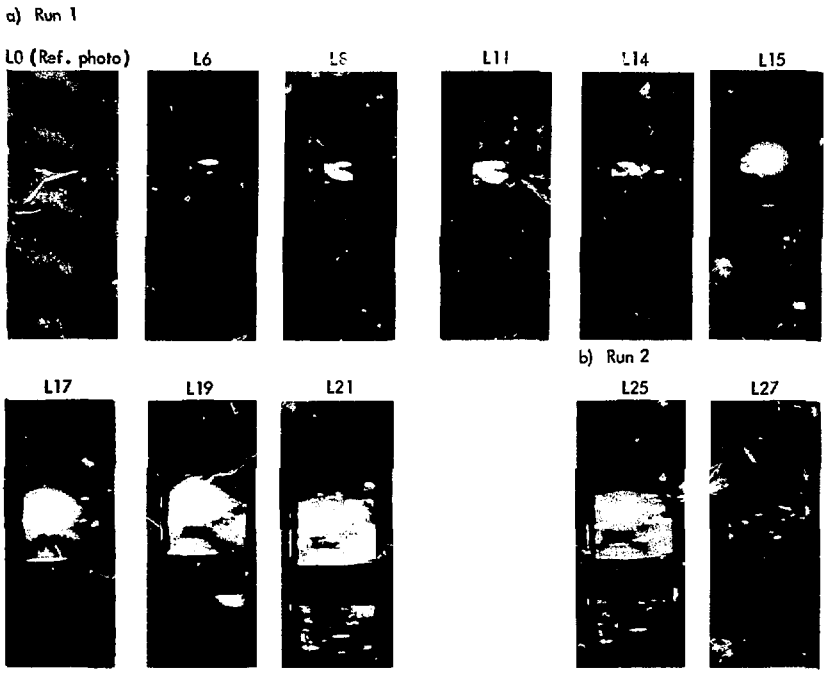

Fig. 23. Projection tube images during tests with implanted 3.2-mil niobium wire. Photograph numbers refer to points on the I-V curves in Fig. 22. A 2-in. dia. projection tube was employed here.

corresponding to the blistered region. [Based on Eq. (1), these spots correspond to a projection height of about 20 μm. This is somewhat larger than the earlier estimate for the height of the blister edges, (about 5 μm), but it is not entirely inconsistent with that observation. The SEM photo is at a poor angle to judge heights, and the edges could also have been pulled up somewhat by the electric field forces.]

The spots appeared to increase in intensity prior to the plateau region, and then break up into multiple spots at L14, the start of the plateau. At L17, the spots were again superimposed to form a very intense spot. Microdischarging suddenly occurred at this point, and while this did not cause complete breakdown, the spot itself was destroyed as seen in photo L19. Note in this photo that new spots tend to ring the area of the original cluster which is now completely dark. Further increase in voltage caused more microdischarging and subsequent formation of many smaller emission spots over a considerable length of the tube. However, photo 21, taken immediately after arc breakdown, indicates that the final breakdown ultimately occurred at the blistered area.

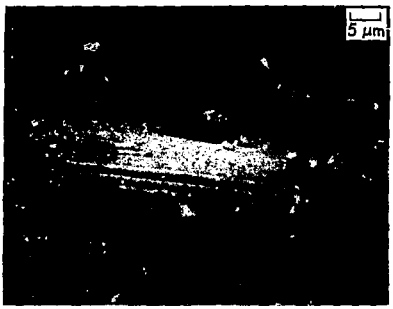

Fig. 24. Scan of blistered and arc region on 3.2-mil niobium (upper photo). Structure in lower photo was found to contain aluminum.

After arc breakdown, run 2 exhibited currents of a magnitude similar to run 1, but without a plateau region. The final breakdown voltage was somewhat higher, and as illustrated by photos L25 and L27, distinct spots associated with the blistered region did not appear again. The experiment was terminated at this point to avoid excessive arc damage prior to SEM studies.

The SEM photograph (Fig. 24) shows rounded "globs" of material near the folded blister edges. Microprobe analysis showed aluminum in these globs, confirming that these structures are the counterparts of the aluminum balls described earlier. The diameter of the prominent "glob" in the lower photograph of Fig. 24 (about 6 μm) is, in fact, comparable to the 1- to 6-μm diameters of the aluminum balls photographed earlier.

A tentative explanation of these observations follows. As pointed out earlier, the folded blister edges have appropriate dimensions for good field emission currents, and this would account for the V-I curve prior to the plateau at 8 kV. The breakup of the spots, combined with the aluminum globs, suggests that microdischarging occurred in the plateau regime. This may have destroyed more prominent blister edges, and in the process formed new emission sites. A multitude of overlapping emission sites grouped together to form the very bright spot in photo L17 of Fig. 23. At this point, an intense microdischarge apparently destroyed a broad region of emission sites in the blistered area, but was not violent enough to cause complete breakdown. Debris from this discharge apparently created new emission sites along unblistered regions of the wire, however, an ultimate breakdown may have well occured there. In fact, a search of the area near the blister site revealed several arc craters of the type shown in Fig. 25. This crater is somewhat larger, but quite similar to the "small" arc craters observed earlier on tungsten (for example, see Fig. 20). It is tempting to postulate that it was initiated by small clumps of debris left on the surface after earlier arcs to the blistered area.

4.2-mil ELECTROPOLISHED NIOBIUM

Current-voltage curves for this test are also shown in Fig. 22, while projection tube images and a pre-breakdown SEM photo are shown in Figs. 26 and 27, respectively.*

The SEM photograph in Fig. 27 indicates rather complete flaking, leaving holes of an average diameter of about 10 μm. This is comparable to the 3.2-mil wire results, but the edges of the blister spots seem smoother. (This may be because the perspective of Fig. 27 makes it hard to see projections near the edges.)

*The SEM photo is actually from a reference wire irradiated simultaneously with the wire used for breakdown studies. Unfortunately, the wire used in voltage tests was broken during insertion into the SEM, making post-mortem studies impossible.

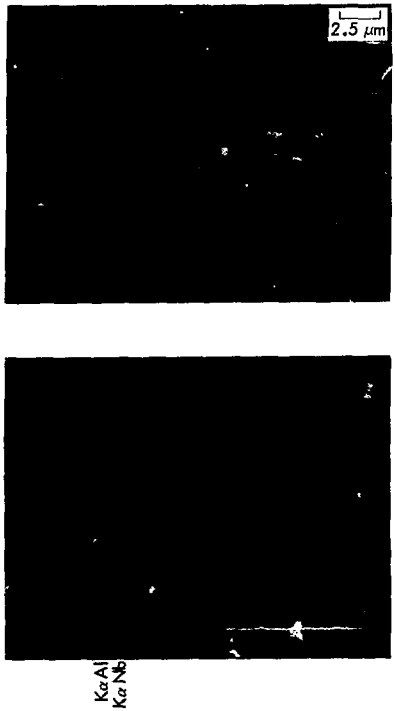

Fig. 25. Arc spot on "clean" (not irradiated) portion of 3.2-mil niobium wire. A bent whisker-ball formation (cf Fig. 17) about 6 μm long is clearly visible. Microprobe (lower photo) shows a trace of aluminum.

This study is not directly comparable to the others reported here for two reasons. First, as already noted, post-mortem SEM photos were not possible, so the actual condition of the surface was not known. Second, in an effort to degas the surface somewhat before voltage testing, this wire was heated at about 700°C for 5-1/2 hours before the test. This was thought to be too low a temperature to affect the actual tests, but there is no proof that it didn't.

The current in the first run exhibited a plateau region (a rapid exponential rise to about 10^{-4} A occured at < 5 kV, not shown in Fig. 22), much like the 3.2 mil wire but starting at lower voltages. After arcing, a semi-plateau still seems to occur, but at much lower currents (around 10^{-7} to 10^{-5} A; see runs 2 and 5 in Fig. 22). In this case, the blister spot was much less distinct during the first run (it is just under the tube holder at the position of the distinct spots in photos M26 through M29 in Fig. 26.)

A bright spot similar to that in M26 was observed (but not photographed) just after arc breakdown during run 1, i.e., just after photo M18. Due to the long image retention time of the fluorescent screen, this is thought to pinpoint the final arc position. This suggests that breakdown indeed occurred at the blistered point rather than at one of the other regions of bright emission observed in photo M18.

This observation appears to be consistent with the type of blistering observed on the following basis. Compared to the 3.2-mil wire (Fig. 28), the present blister area has fewer rough edges that could cause field emission but more clusters of loose material (see Fig. 27). Thus the arc breakdown in the first run may have originated by some loose material leaving the surface rather than by field emission. This would explain the absence of pre-breakdown spots in the blister region.

Once an arc to the blistered region occurred, it could well have created additional emission sites. Subsequent arcs, however, appear to have destroyed surrounding emission sites rather than the blister region itself which remained quite visible throughout the next 5 runs.

6.0-mil ELECTROPOLISHED NIOBIUM

The current-voltage plots for three runs with this wire are shown in Fig. 28 while corresponding image patterns and SEM photographs appear in Figs. 29 and 30, respectively. As seen from Fig. 30, the blisters in this case were just beginning to crack open, so extensive flaking apparently did not occur. (The difference between this and the blisters on the other wires is thought to be due to a difference in temperature which was not controlled during the helium implantation.) In this case, although a definite plateau region occurs in the current-voltage curves for all three runs, an image does not appear at the location of the blister region until photo P17, just before arc

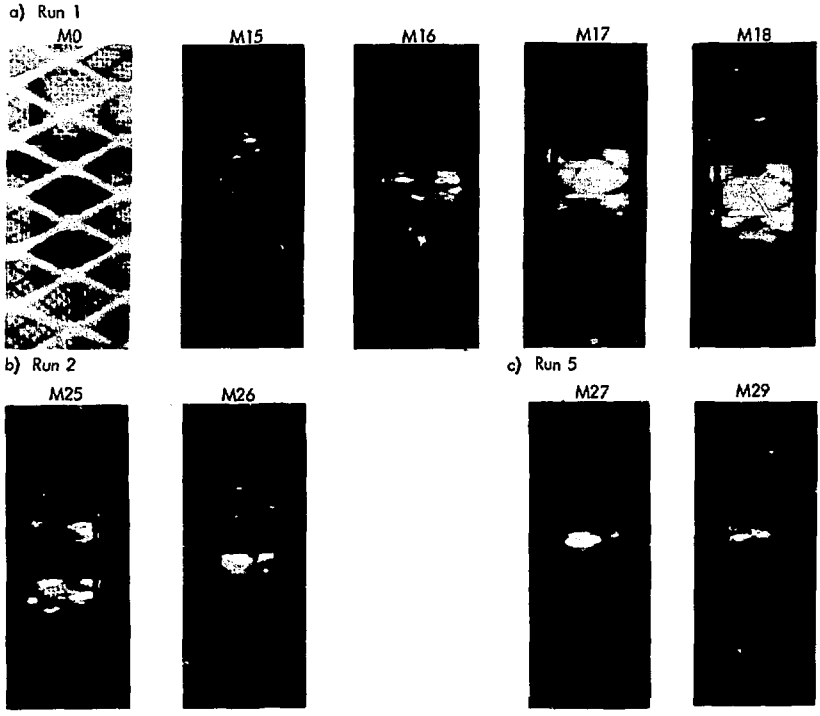

Fig. 26. Projection tube images during tests with 4.2-mil irradiated niobium. Note that the camera location was changed after the first run.

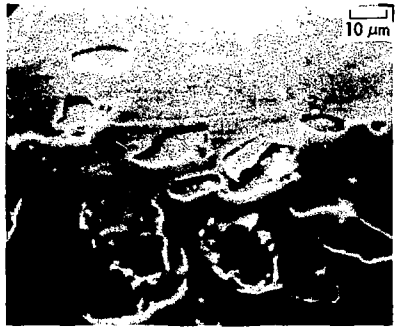

Fig. 27. Flaking on surface of a reference wire irradiated simultaneously with the 4.2-mil niobium wire. Both wires were chemically polished before irradiation. Postmortem photos of the wire tested for breakdown were not made, since it broke during insertion into the SEM.

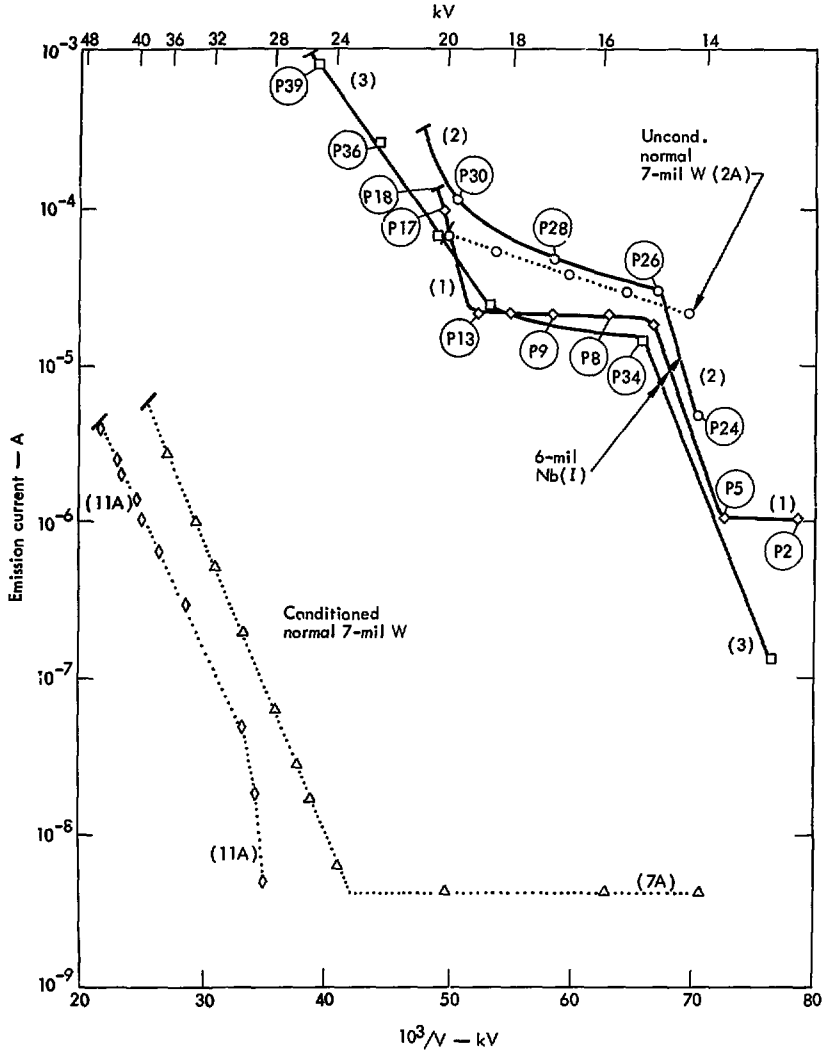

Fig. 28. Current-voltage curves for the irradiated 6-mil niobium wire [Nb(I)]. Three consecutive runs (numbers in parenthesis) are shown. The circled symbols locate point where photos shown in Fig. 29 were taken. For comparison, several runs from normal (not irradiated) 7-mil tungsten wire are shown.

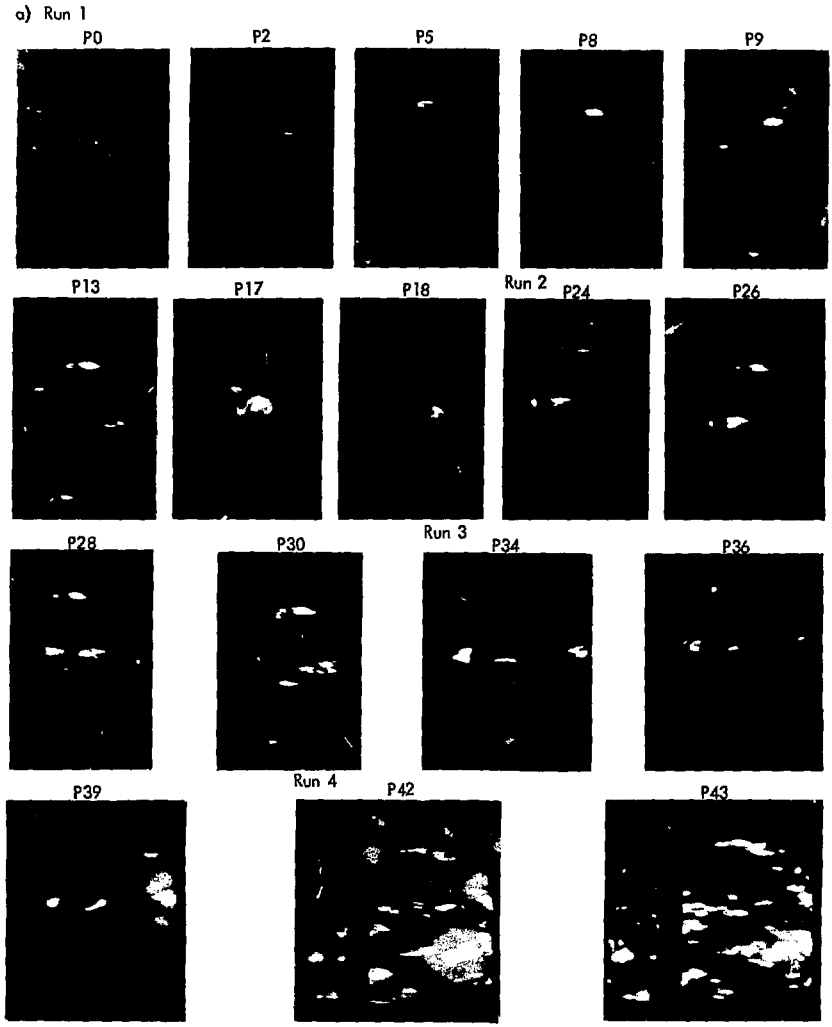

Fig. 29. Projection tube images during tests with blistered 6-mil niobium wire (numbers refer to points designated in Fig. 28, PO is ref. photo). Tests used a 4-in.-diameter projection tube. Note that the camera position was shifted slightly in Runs 3 and 4.

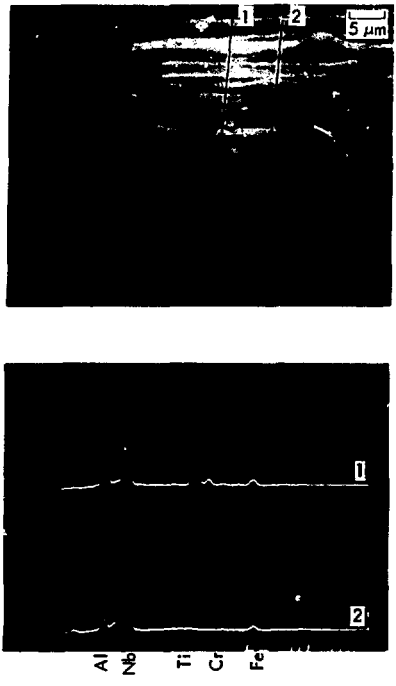

Fig. 30. Arc spot superimposed on blister on irradiated 6-mil niobium wire. Upper trace from microprobe analysis of crater area shows presence of aluminum (vs. standard substrate of lower trace).

breakdown.* Photo P18, taken just after breakdown, shows a lingering image in the blister region, suggesting that the arc occurred there. The fact that the lower voltage photos in this run (P2 – P13) do not show images in the blister area may be because the rounded blisters obtained here do not offer a raised emission site until the field pulls them open further.

The arc crater in Fig. 30 appears to have occurred at a blister site, supporting the idea that serious arcing occurred in this region. The microprobe analysis indicated that the small glob above the crater as well as its lip region contain aluminum. In this case the current-voltage plots retained a plateau for three runs, and indeed the corresponding projection tube photos (P24 – P39) retained image spots in the blister region although their precise location shifted slightly. This persistence would also seem to be consistent with the type of blister involved here. It might be envisioned that the blister tops would be difficult to open via field forces. Those remaining covered after each arc would then be available for opening during subsequent runs. (Contrast this to a flaked surface where the projection and loose debris are present at the start.) By the fourth run (P42 – P43), the blister pattern had finally dispersed, and, as in earlier experiments, a fairly uniform distribution of small spots appeared along a reasonable length of the projection tube.

4.9- AND 5.1-mil ELECTROPOLISHED TUNGSTEN

Unlike niobium, little information is available about blistering of tungsten. Thus these implantations were considered to be exploratory in nature. Indeed, no visible blistering could be observed on the first implanted wire (5.1 mil) when it was removed from the accelerator. It was subsequently run in the high-voltage apparatus, but these tests did not indicate any unusual behavior either. (This does verify that ion bombardment without blistering has a negligible effect on arcing.)

The second 4.9-mil wire did exhibit a definite blister pattern as seen in the SEM photograph of Fig. 31. The difference between the two implantation runs is not clear but may be associated with differences in mounting and location in the ion beam.

In contrast to the earlier flaking on niobium, the damaged area had a melted, porous look, more characteristic of high-temperature bombardment of niobium. We do not know whether this represents a

*The large circular "halo" in the blister region in photo P17 is unique and not observed in other tests. However, based on the bright elliptical images in the upper right of the halo region, Eq. (1) predicts a surface projection $\gtrsim 1$ μm in height. This is roughly an order of magnitude smaller than the height predicted for the flaked blister edges on the earlier 3.2-mil wire (Fig. 25). Indeed, the present rounded blister might be expected to lead to shorter projections.

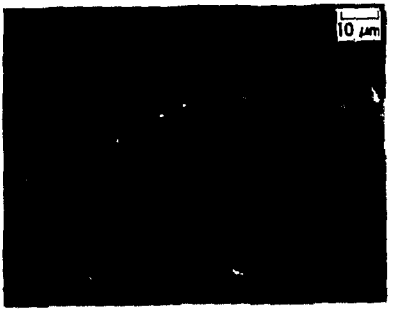

Fig. 31. An arc crater is visible on the edge of blistered spot on 4.9-mil electropolished tungsten wire in upper photo. A closeup of the blistered area is in the lower photo.

fundamental difference between the two materials or a higher temperature during the tungsten implantation.

The current-voltage curves for this wire were included earlier in Fig. 22 while the corresponding projection-tube photographs appear in Fig. 32 with another SEM photograph in Fig. 33.

Again the first breakdown test exhibited a distinct current plateau; however, by run 2, the plateau was not clearly discernible and by run 3, it had completely vanished (see Fig. 22). This behavior is at least in qualitative agreement with the observations from the niobium wires. Thus, it appears that arcing at the end of the first run destroyed any blistered structure that initially caused field emission. This arc occurred at relatively low voltage (about 20 kV), so field-forces may have erected additional blistered structure at around 27 kV during the second run, causing the bright image in S7. As observed with other wires, however, this distinctive structure was quickly destroyed by microdischarging so that subsequent breakdown may well have occurred elsewhere on the wire.

In this case, the blistered area was at the location of the bright image in photos S7 and S8 of Fig. 32. Thus the brightest image during the first run was clearly not associated with the blisters while the lower "ring" of spots in the lower part of photos S1 and S2 are close to (but slightly above) the blistered region. Note that this "ring" of spots has essentially vanished early in the second run before the distinct appearance of the blister image at high voltages (see S7 and S6). Then, as seen from S9 and S10, the bright blister image suddenly broke up just prior to the actual breakdown in run 2. By run 3 (S12 - S18), any distinctive trace of blister spots has disappeared and a bulk of the image spots are in other regions.

It is striking that in both this run and the 6-mil niobium test (where blisters were also present without flaking), the brightest blister-image spots suddenly appeared at high voltage during the second run. In the 6-mil niobium tests, this observation led to the hypothesis that electric field forces erected sections of partly cracked blisters, and this may also be the case here. In contrast, with fully flaked surfaces, there is less chance of a dramatic erection.* While edges of blister holes may be pulled up, this is likely to occur at lower voltages, hence earlier in the experiment.

The arc damage to the blistered area of this wire was quite severe and difficult to interpret due to the rather gnarled character shown in Fig. 33. Rough melted globs, thought to be edges of arc craters, are visible along with what appears to be a small arc

*Fields can play another important role in the case of flaking since, as suggested in the case of the 4.2-mil niobium wire, loose surface material may have been pulled off at higher voltages.

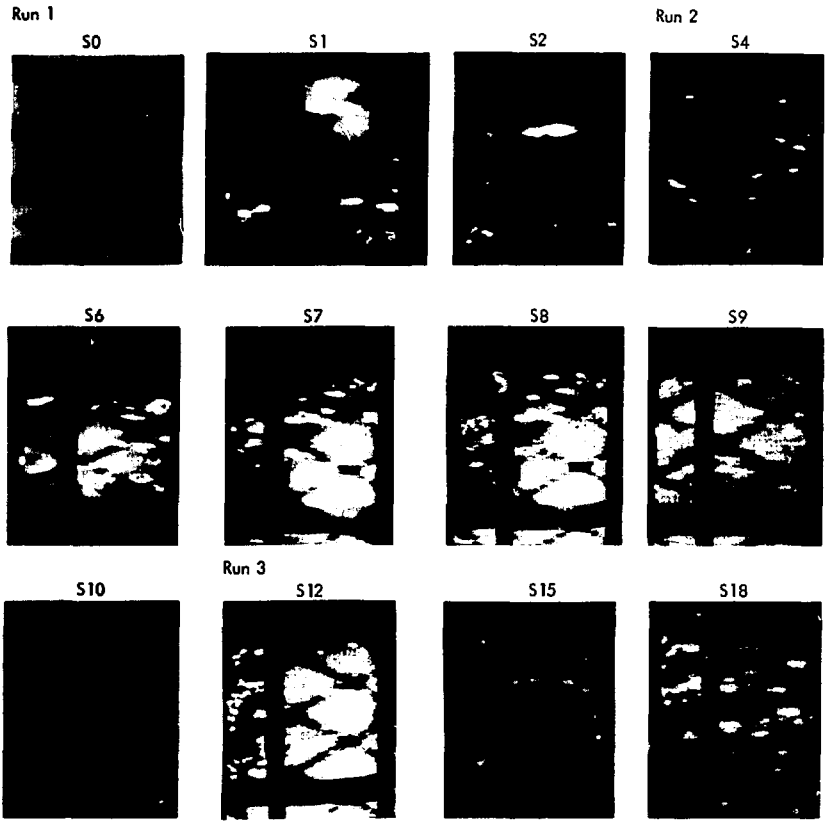

Fig. 32. Projection tube photos for blistered 4.9-mil tungsten wire. A 4-in.-diameter projection tube was employed for these tests. Photo numbers refer to the current voltage plot shown earlier in Fig. 22; P0 is reference photo.

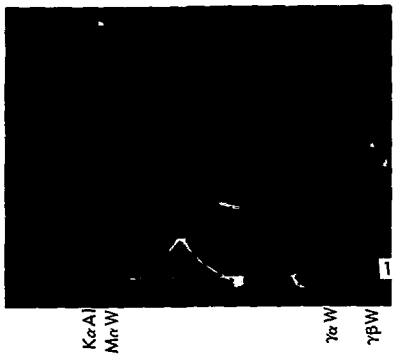

crater (center-left of photo). Even the pit region of the small crater and the melted regions, however, tend to retain a porous structure. This suggests the existence of small helium bubbles throughout the material. Traces of aluminum were again found throughout this region, including the small ball-like structures in the lower center of the photo.

Fig. 33. Closeup of arc damaged area on the 4.9-mil tungsten wire. Microprobe analysis (lower photo) of projection shows presence of aluminum.

Discussion of Blistered Wire Results

The current-voltage curves and projection-tube observations clearly demonstrate that increased field-emission currents occur at the blistered region. The most striking aspect of this is the current plateau illustrated schematically in Fig. 34. It has been postulated that this occurs because the emission current, combined with microdischarging, damages some of the more prominent blister-structures contributing the initial currents. If this did not occur (e.g., if the blistered region were continually being replenished by bombardment), the current might be expected to continue along the dashed line in Fig. 34. In that case, it seems reasonable to assume that the final breakdown would occur at approximately the same current as observed in the plateau case. (Breakdown over a narrow range of currents was found earlier in normal wire experiments[1].) In effect then, as seen from the figure, the plateau phenomena allows a somewhat higher voltage before breakdown.

The breakdown values actually observed, along with lower limits based on the extrapolation described above, are summarized in Fig. 35. Despite the enhanced emission currents obtained with the blistered wires, all of the actual breakdown measurements fall

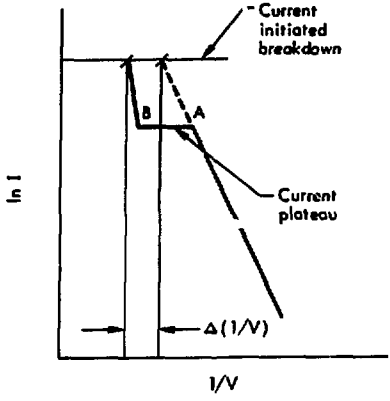

Fig. 34. Schematic illustration of the current plateau regime encountered with blistered wires. It is postulated that the current would follow the dashed line if the blistered area remained intact during emission.

within field emission regime, i.e., between initial and ultimate regime limits defined previously from studies of unblistered tungsten wires[1]. The extrapolated breakdown limits generally fall close to the initial regime limit. From the point of view of grid operation in ion collectors or sources, it is encouraging that even with the latter pessimistic point of view, breakdown from blistering does not fall noticeably below the initial regime.

Some additional data concerning the current plateau for blistered wires is shown in Table 2. With the possible exception of the 4.2-mil Nb wire, the range of electric fields corresponding to the plateau are comparable.

The current densities for the two smaller niobium wires are somewhat larger than for the other two wires. This may be associated with the estimated whisker height in the blistered area. A noticeably larger whisker height was assigned to the 3.2-mil Nb wire, and the corresponding increase in field enhancement could easily account for the large current

Table 2. Plateau Characteristics.

Wire	Plateau Current (A/cm^2)[a]	Average Surface Field[b] (kV/cm)	Est. Whisker Height[c] (cm)
3.2-mil Nb	2.4×10^{-2}	290 - 490	$\sim 2 \times 10^{-3}$
4.2-mil Nb	1.2×10^{-2}	120 - 260	$(\sim 3 \times 10^{-4})$[d]
5.1-mil W	2.0×10^{-3}	200 - 280	$(\sim 5 \times 10^{-4})$[e]
6.0-mil Nb	2.5×10^{-3}	300 - 380	$(\sim 1 \times 10^{-4})$[f]

[a]Normalized to an estimated blister region 0.5 cm long extending half-way around wire.

[b]The range indicated corresponds to points A and B in Fig. 34.

[c]Using Eq. (1) and projection tube images.

[d]From run 5: clear image not visible during first runs.

[e]From run 2; clear image not visible during run 1.

[f]From photo P17 of Fig. 29, just after the plateau of run 1.

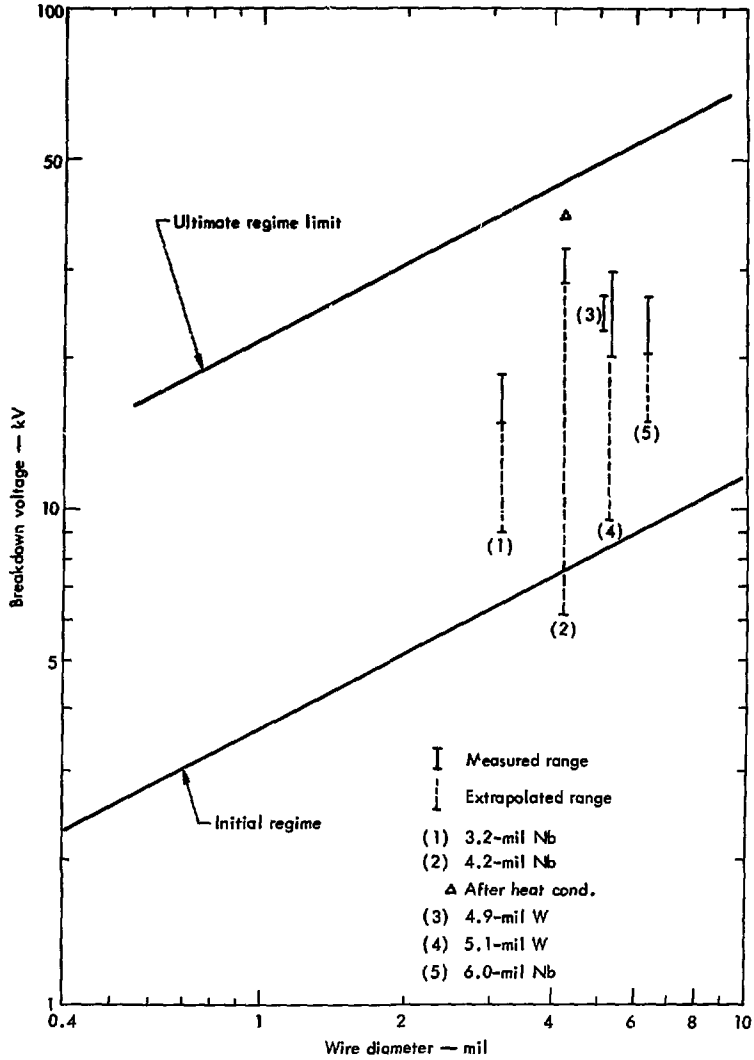

Fig. 35. Voltage breakdown observations for the blistered wires. The range indicated by bars corresponds to values from three or more runs per wire. The dashed line indicated extrapolated values cf Fig. 34. The ultimate and initial curves are from the correlation of Ref. 1.

observed with this wire. The 4.2-mil Nb seems to violate this trend, but the data from this wire is suspect for several reasons. As already discussed, this wire, unlike the others, was heated slightly before testing. Also, breakage prevented post-mortem SEM scans, leaving some uncertainty about blister conditions.

Another encouraging observation relative to device applications is that the blister effect on breakdown appears quite susceptible to conditioning. As seen from Fig. 35, a modest heat treatment pushed the 4.2-mil Nb wire quite close to the ultimate regime limit. Also as seen from the various V-I curves of Fig. 22, a noticeable improvement in performance (i.e., lower currents and high breakdown limits) were obtained after only a few arcs. In several cases (the 3.2- and 4.2-mil Nb), the plateau region was almost eliminated after one run. After two runs, no plateau was visible with the 5-mil wire. While a reduced plateau tended to remain with the 4.2-mil wire after five runs, the critical high-voltage portion of the curve for this wire is well-behaved.

While the present data provide a first insight into possible blister effects on breakdown, considerably more data must be obtained before the problem can be fully evaluated relative to fusion applications. For example, in that case a variety of helium ion energies will be involved resulting in a distribution of blister skin thicknesses (vs. the constant about 1μm in the present case). This could be important since the effective height-to-thickness ratios for the resulting projections would likewise vary, causing different field emission characteristics. Also, grid wires in devices such as direct collectors are expected to run quite hot, resulting in a less distinct, melted blister pattern. It might be hoped that this would be less serious relative to voltage breakdown than the flaked-blisters involved in the present work.*

Continued studies of the present type appear worthwhile to gain more insight into the phenomena involved. Many of the techniques employed can be carried over to the ultimately essential *in situ* tests (i.e., voltage breakdown tests during ion bombardment). In particular, it appears to be feasible to adapt a projection tube for mounting in the irradiation chamber used at Sandia. This would provide a most important diagnostic tool for future studies.

---

*As noted earlier, the blistered region on the 5.1-mil tungsten was somewhat like that expected for high temperatures. If so, this is disappointing in th[illegible]its behavior was not so different from the other wires as might have been anticipated. At this stage, it is difficult to draw general conclusions, since the damage is very sensitive to the material, temperature, and implant conditions involved.

Acknowledgments

Continued suggestions and encouragement by R. W. Moir are most gratefully acknowledged. The generous cooperation W. Bauer, G. Thomas, and D. Morse of Sandia Corporation for helium implantations was indispensible. Discussions with W. Barr, G. Hamilton, and J. Fink were extremely useful, while J. Mitchell provided valuable consultation concerning surface metallurgy.

A number of people worked hard and long so that the experiments could be carried out in the brief time available to the author. J. Kinney, W. Gould, and C. Hansen were instrumental in the design and construction of the apparatus as well as its operation. Their suggestions and help were invaluable. W. Randall, W. Kelly, W. Prokosch, and C. Hansen worked overtime on surface preparation, H. Barnhardt ran high-speed movies and advised on other photography, and W. Kinkaid of EG&G overcame several difficult problems to coat the special projection screens. The SEM photographs were taken by Frank Wittmayer at the LLL electron microscope facility; in addition, several of the original photos of blistered wires were taken at Sandia Corporation by L. E. Brown. Their help is gratefully acknowledged.

References

1. George H. Miley, Voltage Holding Considerations for Direct-Collection Units, Lawrence Livermore Laboratory, Rept., UCRL-51482 (1973).
2. G. H. Miley and R. W. Moir, "Voltage Holding in Direct-Collectors," in: Proc. Fifth Symposium on Engineering Problems of Fusion Research, (Princeton, 1973).
3. R. W. Moir, W. L. Barr, and G. H. Miley, J. Nuc. Materials, 53, 86-96 (1974).
4. Details of the processes are discussed in a letter from R. M. Kinkaid (EG&G) to J. D. Kinney (LLL) dated July 9, 1974 and referenced as CRI-75-01.
5. I. Brodie and I. Weissman, Vacuum, 14, 299-301 (1964).
6. J. J. Maley, J. Vacuum Science, 8, 697-700 (1971).
7. I. Brodie, J. Appl. Phys., 35, 2324-2332 (1964).
8. D. K. Davies and M. A. Biondi, J. Appl. Phys., 39, 2979-90 (1968).
9. D. K. Davies and M.A. Biondi, J. Appl. Phys., 41, 88-93 (1970).
10. W. Bauer and G. J. Thomas, J. of Nucl. Mat., 53, 127-133 (1974).

Appendix A: Comments About Applications of Breakdown Criteria to Ion Source Design

As pointed out by several authors, voltage breakdown represents a key factor in the scaling of ion sources using single stage extraction from a plasma. (e.g., see Refs. A1 - A3). This is easily demonstrated as follows: if the emitting surface can be approximated by a plane diode with a spacing (or distance between the plasma and extraction grids) of d, the extracted current density j due to extraction voltage V will follow Langmuir-Child's space-charge law, i.e.

$$j = c\, V^{3/2}/d^2, \qquad (A1)$$

where c is a constant.

As shown earlier,[A4] the voltage breakdown limit V_b for the grid is approximately given as:*

$$V_b \approx K_j\, d^{1/2} \qquad (A2)$$

where K_j is an appropriate constant describing the breakdown regime involved. Thus, from Fig. 15 of Ref. A4, we have

$$K_j = \begin{cases} 302 & \text{(ultimate regime)} \quad (A3) \\ 48.8 & \text{(initial regime)} \quad (A4) \end{cases}$$

where d is in cm and V_b is in kV.

*This assumes ideal vacuum breakdown. The effect of bombardment of the surface by stray ions and electrons as well as x-rays must be investigated before a more precise correlation is possible. What may be more important is that if small diameter grid wires are used for extractors, the enhancement of the electric field at their surface (vs. the ideal plane electrode assumed here) must be considered. Note that the correlation of Ref. 1 gives $V_b \sim K_j y^{1/2}$ where y is the voltage to surface field ratio.

Combining Eqs. (A1) and (A2), we obtain the maximum current j_m that can be extracted before voltage breakdown as

$$j_m \approx C\, K_j^4\, V^{-5/2}. \qquad (A5)$$

A plot of this relation is shown in Fig. A1.

The maximum current density decreases rapidly with extraction voltage. Equally significant is the strong dependence of j_m on the breakdown constant K_j [recall the 4th power in Eq. (A5)]. Thus, if 100-kV operation is desired (a nominal target for near-fusion applications), Fig. A1 indicates that a current density of only about 0.08 A/cm^2 could be obtained with operation at the initial regime limit, while a full 10 A/cm^2 could be delivered if it were possible to use conditioning techniques to achieve the ultimate regime limit. Clearly, a strong motivation exists to achieve some conditioning such that operation beyond the initial regime is possible.

For perspective, an estimate of the operating line for current experimental devices is included in Fig. A1. (This is based on data in Refs. A1 and A5 where current densities of order of 0.5 A/cm^2 at 30 kV are reported.) Based on this, it appears that problems such as ion bombardment and geometrical factors have limited present sources to operation even lower than that predicted by the initial regime correlation of Ref. A4. One problem with these designs is that it is not possible to use inplace heating techniques to condition the grids. Rather, conditioning is achieved through a lengthy break-in procedure involving actual operation on a test stand.[A6] The adequacy of this technique is not clear, and certainly, as suggested by Fig. A1, there is a stong motivation to develop better conditioning.

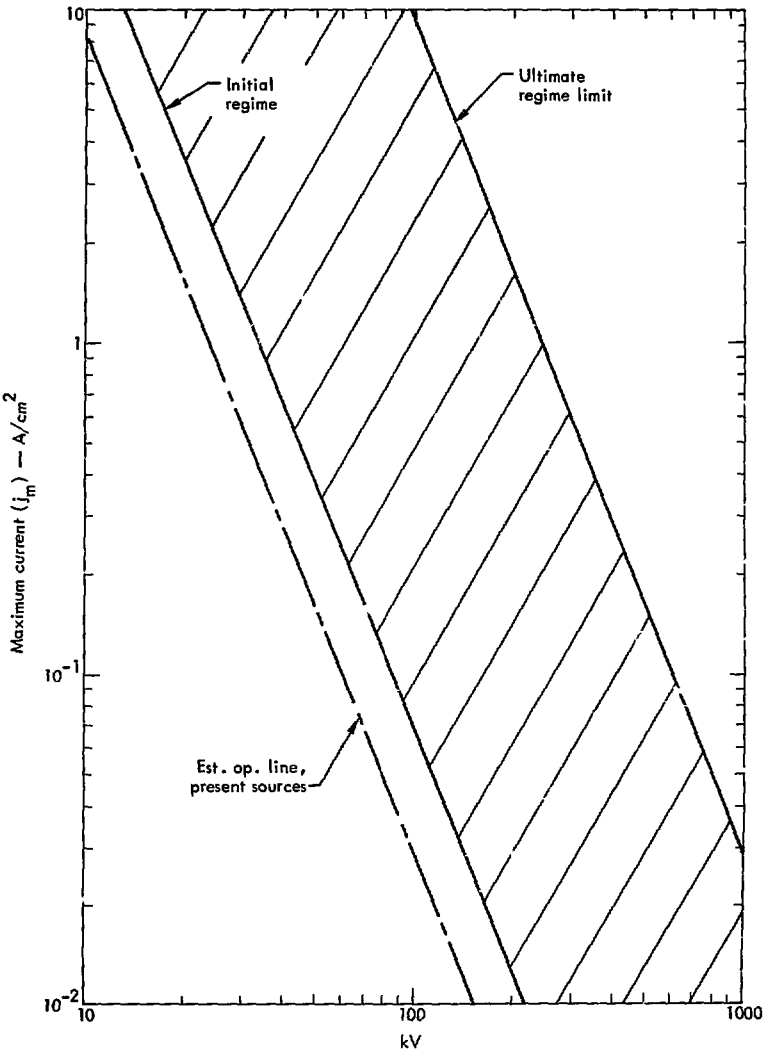

Fig. A1. Current-voltage characteristics for a single-stage extraction of ion currents for a plasma source.

References

A1. E. Thompson, "The Ion Optics of a Single Stage Post-Acceleration System." Proc. 2nd Sym. on Ion Sources and Formation of Ion Beams, Berkeley, Calif., Oct. 1974. pp II-7-1 to 7-4.

A2. D. R. Sweetman, "Neutral Injection Heating," Sym. on Plasma Heating and Injection, Varenna-Villa Monastero, Italy, Oct. 1972. pp 117-119.

A3. G. W. Hamilton, W. L. Dexter, and B. H. Smith, A Design Study of a Neutral Injection System for FERF, Lawrence Livermore Laboratory, Rept., UCRL-75547 (1974) pp 7-8.

A4. G. H. Miley, Voltage Holding Considerations for Direct-Collection Units, UCRL-51482 (1973).

A5. W. Bauer, et al., Neutral Beam Sources: Applications in Science and Technology, Sandia Laboratories, Livermore, Calif., Rept. SSL-74-8204 (1974).

A6. E.B. Hooper, Lawrence Livermore Laboratory, private communication (August 1974).

Appendix B: Emission Currents from a Shaped Molybdenum Electrode used in a MATTS-Type Ion Source

During this study, considerable difficulty was encountered with arcing in experimental MATTS-type ion-source modules under development to provide 10-A, 25-kV beams. The difficulty was thought to originate with the new "Duffy-type" plasma and extraction electrodes employed. However, visual observations were not possible during operation, so the origin of the arcing could not be definitely established. To obtain some preliminary information, a molybdenum electrode was run in the projection tube. This particular electrode was selected because its odd shape, illustrated in Fig. B1, suggested that it might be involved in the arcing. (The other extraction electrodes consisted of normal tungsten grid wires.) The electrode used was taken directly off the source assembly line.* Cleaning fluid was used to remove oils by drawing the electrode through appropriate dies. Otherwise, no special surface treatment was attempted prior to mounting in the source, actual source operation being employed for conditioning. Thus, as illustrated in the SEM photos of Fig. B2, the surfaces on these electrodes are typically very rough.

*The cooperation and help of T. J. Duffy in this study is gratefully acknowledged.

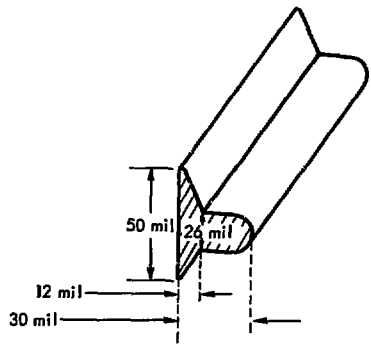

Fig. B1. Cross-section of the molybdenum electrode. The odd shape is necessary to aid in focusing of the extracted ion beam.

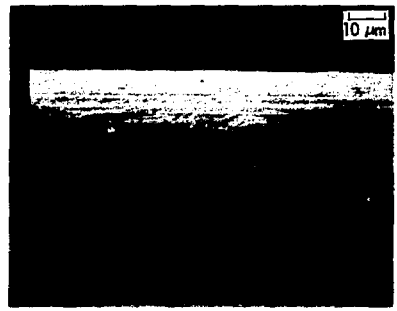

Fig. B2. Photos of surface of a standard molybdenum electrode prior to voltage testing. As seen from the closeup, the dark spots in the upper photo are actually valleys due to the rough finish.

As might be anticipated, the emission patterns observed with this electrode were largely concentrated in a line along the two protruding edges (Fig. B1). As with normal wires, individual images on the projection tube were elliptical. The most unique aspect observed was a fairly common appearance of vertical streaks that moved with voltage changes. (Similar streaks were occasionally observed with wires, but not nearly so often.)

After several arcs had occurred, the electrode was sectioned at the location of several bright image spots and examined in the SEM. Projections located on this surface are shown in Figs. B3 and B4.

The massive (about 100 μm long X 10 μm diam.) whisker in Fig. B3 occurred along a sharp edge of the electrode. As in other experiments, the ball-like objects on it contain aluminum from the anode. Calcium silicate was also detected, indicating transport of phosphor material from the projection screen along with the aluminum. Thus, it seems certain that this whisker was involved invigorous emission currents and possibly suffered an arc. Its location and appearance

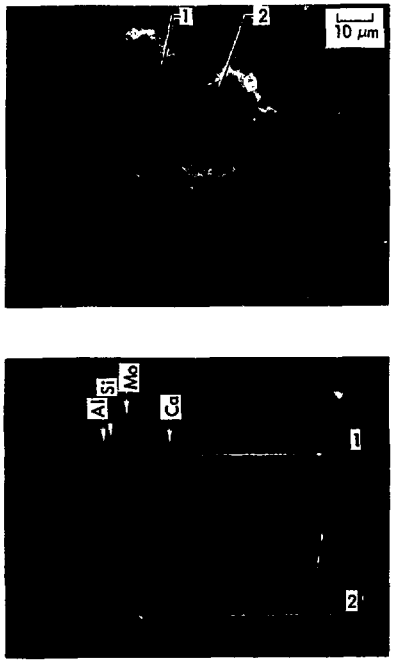

Fig. B3. Large projection located on the edge of the standard moly grid (1K enlargement). Analysis on ball formation (upper trace of microprobe) shows telltale presence of aluminum and calcium, indicating arcing.

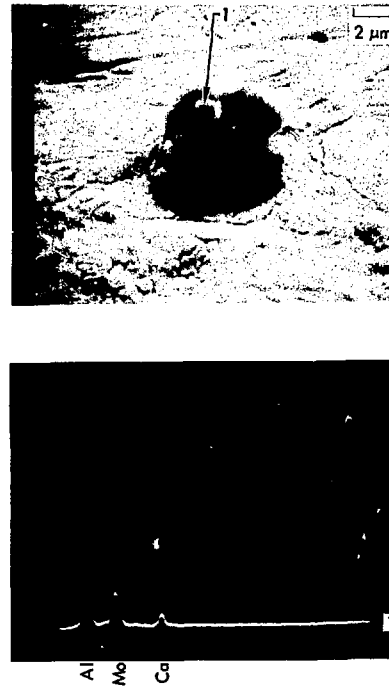

Fig. B4. Another type of surface projection on the molybdenum electrode. The ball on the surface contains large amounts of aluminum as shown by the microprobe trace.

suggest that it may have been pulled up from the surface by field forces. In fact, it might be expected that the edges of the electrode would be prone to such erections due to damage caused during manufacture and forming. While there is no direct evidence, it might be guessed that such formations are associated with the moving vertical streaks observed on the image tube as described earlier.

A second projection found on the surface is shown in Fig. B4. This projection appears to be growing (or pulled) out of the surface, and again a telltale aluminum ball identifies it as an emission site.

In conclusion, the molybdenum electrode appears to be quite prone to field erection of large whiskers and other projections. This could be a characteristic of molybdenum, but it is more probably due to the machining techniques used to shape the grid. Further studies are necessary to fully understand the problem and to find ways to prevent it.